International Journal of Modern Physics B, Vol. 16, Nos. 1 & 2 (2002) 383–390

COMPARTMENTAL MODELING OF MULTIDIMENSIONAL CRYSTALLIZATION

DAVID L. MA, RICHARD D. BRAATZ

Chemical Engineering, University of Illinois, 600 South Mathews Avenue, Box C-3 Urbana, Illinois 61801, United States of America

DANESH K. TAFTI

National Center for Supercomputing Applications, 4165 Beckman Institute Urbana, Illinois 61801, United States of America

Received (10 June 2001)
Revised (15 September 2001)

An approach that couples compartmental modeling with high resolution methods is developed to simulate spatial variations in the crystal size and shape distribution in solution crystallization processes. This is the first time that compartmental modeling has been applied to a crystal system with multiple characteristic length scales. The compartment model enables a more accurate modeling of the effect of secondary nucleation, which is key to accurately predicting the crystal size distribution of the final product. A parallel implementation of the numerical algorithm results in short computation times.

1. Introduction

Crystallization from solution is an industrially important unit operation due to its ability to provide high purity separations. For efficient downstream operations (such as filtration and drying) and product effectiveness (e.g., bioavailability, tablet stability), predicting the crystal size distribution and morphology can be critically important. This is especially true for the multidimensional (e.g., needle-like) biochemical crystals produced in the pharmaceutical industry. Increased competition in the pharmaceutical industry has motivated an interest towards understanding and controlling crystallization processes.[1,2]

The characteristics of the product crystals are determined internally by the given solvent-solute system and externally by the environment that the crystals experience. Crystals are not distributed uniformly in most industrial crystallizers. Such deviations from perfect mixing must be considered in the modeling of crystallization processes in which physical phenomena such as aggregation, attrition, or secondary nucleation occur. The approach proposed in this paper, which couples compartmental modeling with high resolution methods, can efficiently simulate the crystal size and shape distribution to high accuracy while taking spatial variations

into account. The crystallizer is subdivided into a finite number of compartments, in which uniform conditions are assumed in each compartment. Each compartment has input and output streams that share flows with its neighbors. The characteristics and quantity of crystals in the streams are governed by the local conditions. It will be shown that the compartmental model enables a much more accurate modeling of the effects of secondary nucleation, which is the dominant mechanism for producing new crystals in most seeded batch crystallizers. By not requiring the full solution of the fluid and particle momentum equations, the approach is computationally feasible using today's computer hardware. A parallel programming implementation further reduces the simulation time.

Another contribution of this paper is the development of a high resolution finite difference algorithm for simulating multidimensional crystallization processes. High resolution algorithms are applicable to hyperbolic equations and have been used to simulate shock waves and to solve the Boltzmann equation for rarefied gases.[3,4] The algorithms provide second-order accuracy without the undesirable oscillations that naive second-order methods usually exhibit when applied to hyperbolic equations, while also eliminating numerical diffusion demonstrated by first-order methods.

The paper is organized as follows. The model of a well-mixed batch multidimensional crystallizer is presented first, followed by a description of compartmental modeling, the high resolution algorithm, results, and discussion.

2. Multidimensional Crystallization: Well-Mixed Case

While the following description of multidimensional crystallization is rather general, potassium dihydrogen phosphate (KH_2PO_4, KDP) is used to illustrate the key ideas. The shape of KDP crystals is tetragonal prism in combination with tetragonal bipyramid, and the angle between the prism sides and pyramid faces is 45°.[5] The two internal dimensions r_1 and r_2 are the width and length of the KDP crystal, respectively (see Figure 1). Accordingly, the volume of a single crystal is

$$V_c = \frac{1}{3} r_1^3 + (r_2 - r_1) r_1^2. \tag{1}$$

For a well-mixed batch crystallizer in which the crystals have two characteristic length scales, the process is described by the population balance equation:[6,7]

$$\frac{\partial f}{\partial t} + \sum_{j=1}^{2} \frac{\partial \{G_j[c(t), T(t)] f\}}{\partial r_j} = h(t) \tag{2}$$

where f is crystal size distribution, r_j refers to each characteristic length scale, G_j refers to the growth rate for the j^{th} length scale, c is the solute concentration, and h describes the crystal creation mechanisms which can be a function of the crystal size distribution, the solute concentration, and the temperature.

The growth rates G_1 and G_2 are functions of the solute concentration c and the saturated solute concentration c_{sat}. For KDP these equations are:

$$G_1 = k_{g1} S^{g1} \tag{3}$$

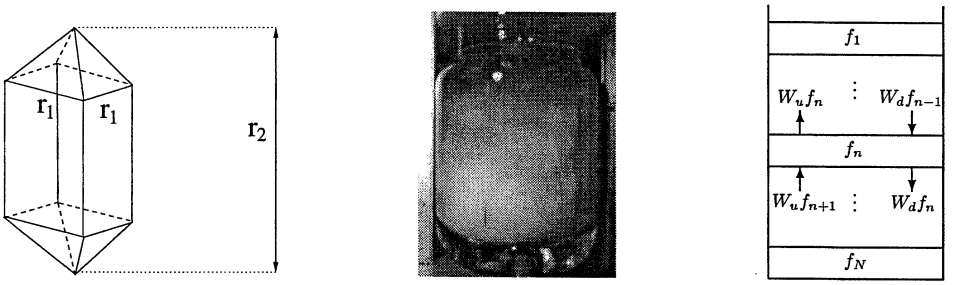

Fig. 1. A KDP crystal, a batch laboratory crystallizer, and its simulation model with N compartments

$$G_2 = k_{g2} S^{g_2}, \tag{4}$$

where $S = (c - c_{\text{sat}})/c_{\text{sat}}$ is the relative supersaturation and g_1, g_2, k_{g1} and k_{g2} are kinetic parameters. The saturated solute concentration c_{sat} for KDP is given by[8]

$$c_{\text{sat}} = 9.3027 \times 10^{-5} T^2 - 9.7629 \times 10^{-5} T + 0.2087, \tag{5}$$

where T is the temperature in Celsius. Secondary nucleation is the dominant mechanism for producing new crystals in most seeded batch crystallizers. This type of nucleation kinetics is usually characterized as being proportional to either the area or volume of crystals in the crystallizer. In this paper, the latter is assumed:

$$h(t) = k_b \left(\frac{c - c_{sat}}{c} \right)^b \int_0^\infty \int_0^\infty f(r_1, r_2, t) V_c(r_1, r_2)\, dr_1\, dr_2. \tag{6}$$

A solute mass balance completes the model for a batch crystallizer. With the assumption that nucleated crystals have negligible size (a good assumption in practice), the amount of solute leaving the solution must be accounted by crystal growth. For KDP this equation is

$$\frac{dC}{dt} = -\alpha \int_0^\infty \int_0^\infty f(r_1, r_2, t)(2G_1(r_1 r_2 - r_1^2) + G_2 r_1^2) dr_1 dr_2 \tag{7}$$

where α is the geometric-stoichiometric constant chosen so that the right hand side of the equation has the correct units. Table 1 summaries the parameter values in (3) to (6), which were determined using parameter estimation and model-based experimental design.[9,10,11,12]

3. Compartmental Modeling

Perfect mixing is rarely valid in practice. A 2-liter batch crystallizer is shown in Figure 1. The crystal size distribution f varies substantially along the height of the crystallizer. Due to gravity, most crystals stay at the bottom of the crystallizer, while smaller crystals tend to flow with the water and can be seen in the middle and upper regions. Few crystals are located near the top of the slurry.

Table 1. Kinetic parameters determined from laboratory data

Parameters	Values	Units
g_1	1.48	dimensionless
k_{g1}	12.21	$\frac{\text{micron}}{\text{second}}$
g_2	1.74	dimensionless
k_{g2}	100.75	$\frac{\text{micron}}{\text{second}}$
b	2.04	dimensionless
k_b	7.49×10^{-8}	$\frac{\text{particles}}{\text{micron}^3\ \text{second}}$

Compartmental modeling has been used to take spatial variations into account in one-dimensional crystallizers.[1,13] As suggested from Figure 1, the crystallizer can be subdivided into smaller compartments. Each compartment is assumed to be well-mixed, that is, the nucleation and growth kinetics are uniform throughout the compartment, and consequently a variation on (2) can be applied to each compartment. The amount of crystals and the crystal size distribution f may be different in each compartment.

Using a larger number of compartments can result in a more accurate model of the system. Each compartment has input and output streams that share flows with its neighbors. The crystal size distribution in those streams is governed by the local conditions. The smallest crystals will flow along streamlines; therefore, the distribution for the smallest crystals in the output streams of the n^{th} compartment should be equal to the distribution inside the n^{th} compartment. On the other hand, the downward output stream of the n^{th} compartment will have bigger crystals than the upward output stream, when the crystals have a higher density than the fluid. Two weighting functions W_d and W_u are used to characterize these distributions. The crystal size distributions are $W_d f_n$ and $W_u f_n$ in the downward and upward output streams of the n^{th} compartment, where f_n is the crystal size distribution in the n^{th} compartment and

$$W_u = 1.0 - \frac{\beta_1 r_1}{\max(r_1, r_2)} - \frac{\beta_2 r_2}{\max(r_1, r_2)}, \tag{8}$$

$$W_d = 1.0 + \frac{\beta_1 r_1}{\max(r_1, r_2)} + \frac{\beta_2 r_2}{\max(r_1, r_2)}. \tag{9}$$

The constants β_1 and β_2 are determined from experiments, and r_1 and r_2 are the characteristic length scales for the crystals. For the n^{th} compartment, the population balance equation is

$$\frac{\partial f_n}{\partial t} + \sum_{j=1}^{2} \frac{\partial\{G_j[c(t), T(t)] f_n\}}{\partial r_j} = h(t) + \frac{F}{V_n}(W_d f_{n-1} + W_u f_{n+1} - W_u f_n - W_d f_n) \tag{10}$$

where F is the flow rate of input and output streams, and V_n is the volume of the compartment n. A high resolution algorithm that solves this system of partial differential equations is discussed next.

4. High Resolution Algorithm

The population balance equation (10) is a multidimensional hyperbolic equation whose solution confounds many first-order and second-order finite difference algorithms due to the sharp variations of its solution with respect to the characteristic crystal dimensions. In the literature, first-order methods are often used with special consideration of mesh size in order to reduce numerical diffusion.[14] Higher order methods can give oscillatory solutions, which for crystallization processes result in a crystal size distribution with negative values, which are not physically realistic.

High resolution methods have been developed that can effectively handle large gradients in the solution while retaining second-order accuracy.[3,15,16,17,18] High resolution methods have been mostly developed for the 1D wave equation. For the 2D wave equation (10), the direct application of a high resolution method gives only first-order accuracy.[19] To solve (10) to second-order accuracy, a splitting method is first applied to decompose its homogeneous equation into a pair of 1D equations. Then a high resolution method is applied to solve each 1D equation. After the homogeneous equation is solved for time step k, the source term is added to the corresponding compartments over the same time increment.[16]

5. Results and Discussion

The parameters for a batch crystallizer are reported in Table 2. The temperature is assumed to be uniform throughout the crystallizer, with each compartment having the temperature profile in Figure 2.

Table 2. Parameters used in simulation

Variable	Description	Value	Units
k	time step	1	second
h	mesh size	1	micron
F	flow rate	10	cm^3/second
V	volume	2	liter
t	batch time	2	hour
β_1	coefficient	0.1	dimensionless
β_2	coefficient	0.1	dimensionless

Increasing the number of compartments makes the simulation time longer if only a single processor handles all the computations. Parallel programming was used to reduce the simulation time. Each compartment was assigned to a different processor. The task for each processor was to compute the solute concentration and crystal size distribution in the compartment that it was assigned and then pass this information to its neighbors (the upper and lower compartments). Since the computation is done in parallel, the simulation time can be nearly independent of the number of compartments. However, the simulation time does increase somewhat as compartments are increased because it takes time to pass the information to

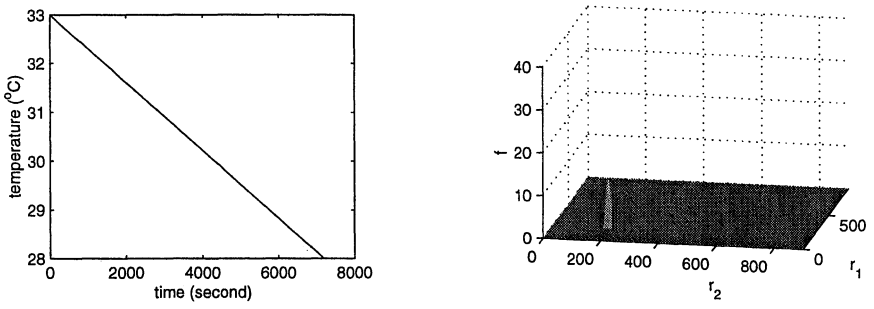

Fig. 2. Temperature profile of the batch crystallizer and initial seed crystal size distribution in the bottom compartment. The average characteristic length scales for the seed are 180 microns.

the neighbors. Table 3 shows the simulation time when different numbers of compartments were used. The simulation time increases 15-25% when the number of compartments doubles.

Table 3. Simulation time for different numbers of compartments. The simulations were done on 64 HP Kayak Visualize Workstations, each with dual PIII Xeon 550 MHz processors, 512k cache per cpu, and 1GB of memory.

compartments	4	8	16	32	64
time (min)	67	77	94	118	131

As shown in Figure 3, the relative supersaturation at the top of the crystallizer can be five times higher than at the bottom. This implies that crystals grow faster in the upper compartments. As the crystals become larger, they tend to leave the top compartments due to gravity and enter the bottom compartments which are associated with slower growth rates. At the same time, fresh smaller crystals enter the top compartments from the bottom. Due to the different growth rates and circulation inside the crystallizer, the final crystal size distribution is very different from that computed assuming a well-mixed batch crystallizer (figure not shown due to space limitations). Significantly larger crystals are produced when spatial variation is taken into account.

Before crystallization starts, seed crystals are added to the solution to avoid spontaneous nucleation from solution. The crystal size distribution as various positions in the crystallizer at the end of the batch run is shown in Figure 4. Most of the crystals are located at the bottom of the crystallizer, which is also where most of the secondary nucleation occurs. This suggests that the existing models that assume uniform nucleation throughout the crystallizer do not adequately model this phenomena for most batch crystallizers.

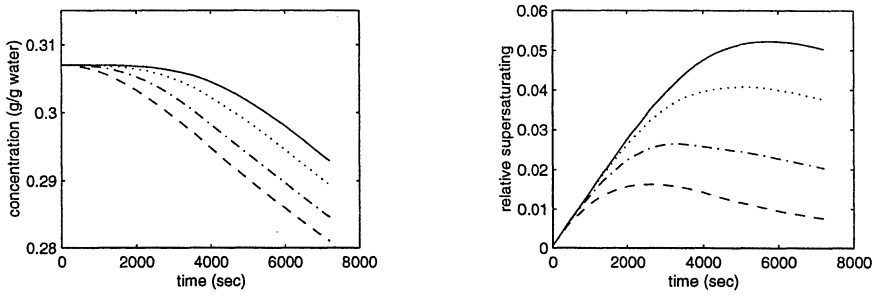

Fig. 3. Concentration and relative supersaturation profiles when 64 compartments are used. The compartments are numbered starting from the top of the crystallizer. The compartment numbers are: 64 (- - -), 48 (- · -), 32 (· · ·), 16 (—).

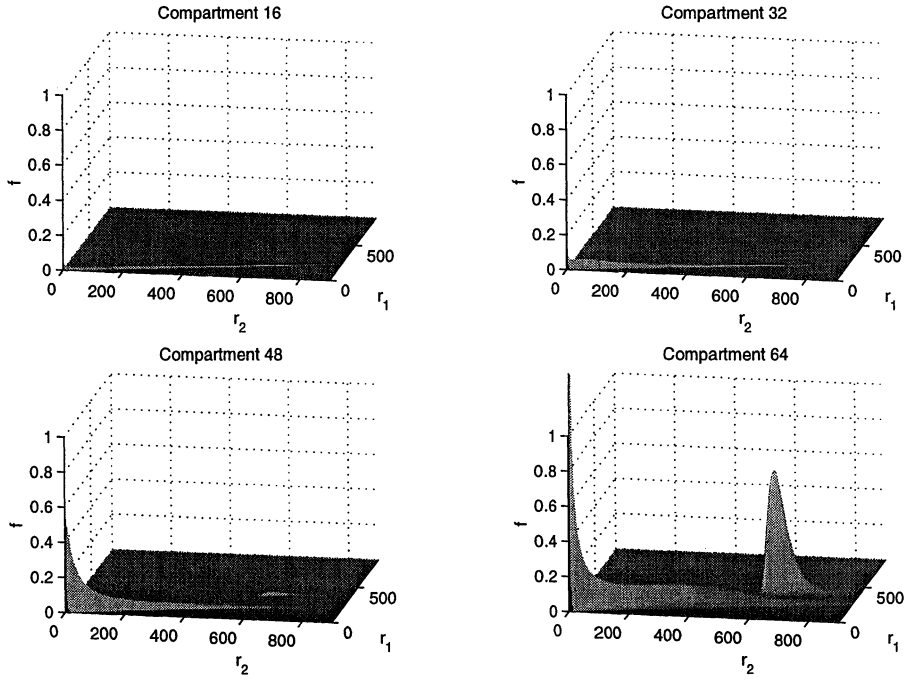

Fig. 4. Final crystal size distribution when 64 compartments are used. The distribution of crystals grown from seed is located to the right in compartment 64. The distribution of crystals initiated from secondary nucleation is the ridge starting from the origin.

6. Conclusion

Compartmental modeling was coupled with a high resolution algorithm to simulate the dynamics of a batch multidimensional crystallizer. The simulation results show that the crystal size distribution and solute concentration significantly vary along

the height of the crystallizer. The results also show that the secondary nucleation rate is much larger at the bottom of the crystallizer, and the growth rate is much larger at the top. The high resolution method provides very satisfactory results. No spurious oscillations or numerical diffusion occurred. Parallel programming made it possible to have short simulation times while using a large number of compartments.

Acknowledgements

Support from the National Center for Supercomputing Applications and the Computational Science and Engineering Program at the University of Illinois is gratefully acknowledged.

References

1. R. D. Braatz and S. Hasebe, in *Chemical Process Control VI*, ed. J. B. Rawlings and B. A. Ogunnaike (AIChE Press, New York, 2001), in press.
2. T. Togkalidou, R. D. Braatz, B. Johnson, O. Davidson and A. Andrews, *AIChE J.* **47**, 160 (2001).
3. R. J. LeVeque, *Numerical Methods for Conservation Laws* (Birkhäuser Verlag, Basel, Germany, 1992).
4. J. Y. Yang, J. C. Huang and L. Tsuei, *Proc. Royal Soc. London A* **448**, 55 (1995).
5. J. W. Mullin and A. Amatavivadhana, *J. Appl. Chem.* **17**, 151 (1967).
6. H. M. Hulburt and S. Katz, *Chem. Eng. Sci.* **19**, 555 (1964).
7. A. Randolph and M. A. Larson, *Theory of Particulate Processes* (Academic Press, San Diego, 1988).
8. T. Togkalidou, M. Fujiwara, S. Patel and R. D. Braatz, *J. Cryst. Growth* (2001), **231**, 534 (2001).
9. S. H. Chung, D. L. Ma and R. D. Braatz, *Can. J. Chem. Eng.* **77**, 590 (1999).
10. S. H. Chung, D. L. Ma and R. D. Braatz, *Chemom. Int. Lab. Sys.* **50**, 83 (2000).
11. D. L. Ma, S. H. Chung and R. D. Braatz, *AIChE J.* **45**, 1469 (1999).
12. H. B. Matthews and J. B. Rawlings, *AIChE J.* **44**, 1119 (1998).
13. H. J. M. Kramer, J. W. Dijkstra, A. M. Neumann, R. O. Meadhra and G. M. van Rosmalen, *J. Crys. Growth* **166**, 1084 (1996).
14. K. Sotowa, K. Naito, M. Kano, S. Hasebe and I. Hashimoto, *J. Process Contr.* **10**, 203 (2000).
15. A. Harten, *J. Comp. Phys.* **49**, 357 (1983).
16. R. J. LeVeque, *J. Comp. Phys.* **131**, 327 (1997).
17. S. Osher and S. Chakravarthy, *SIAM J. Numer. Anal.* **21**, 955 (1984).
18. P. K. Sweby, *SIAM J. Numer. Anal.* **21**, 995 (1984).
19. J. B. Goodman and R. J. LeVeque, *Math. Comput.* **45**, 15 (1985).